Unveiling the effects of berenil, a DNA-binding drug, on Trypanosoma cruzi: *implications for kDNA ultrastructure and replication*

Aline Araujo Zuma, Danielle Pereira Cavalcanti, Marcelo Zogovich, Ana Carolina Loyola Machado, Isabela Cecília Mendes, et al.

Parasitology Research
Founded as Zeitschrift für Parasitenkunde

ISSN 0932-0113

Parasitol Res
DOI 10.1007/s00436-014-4199-8

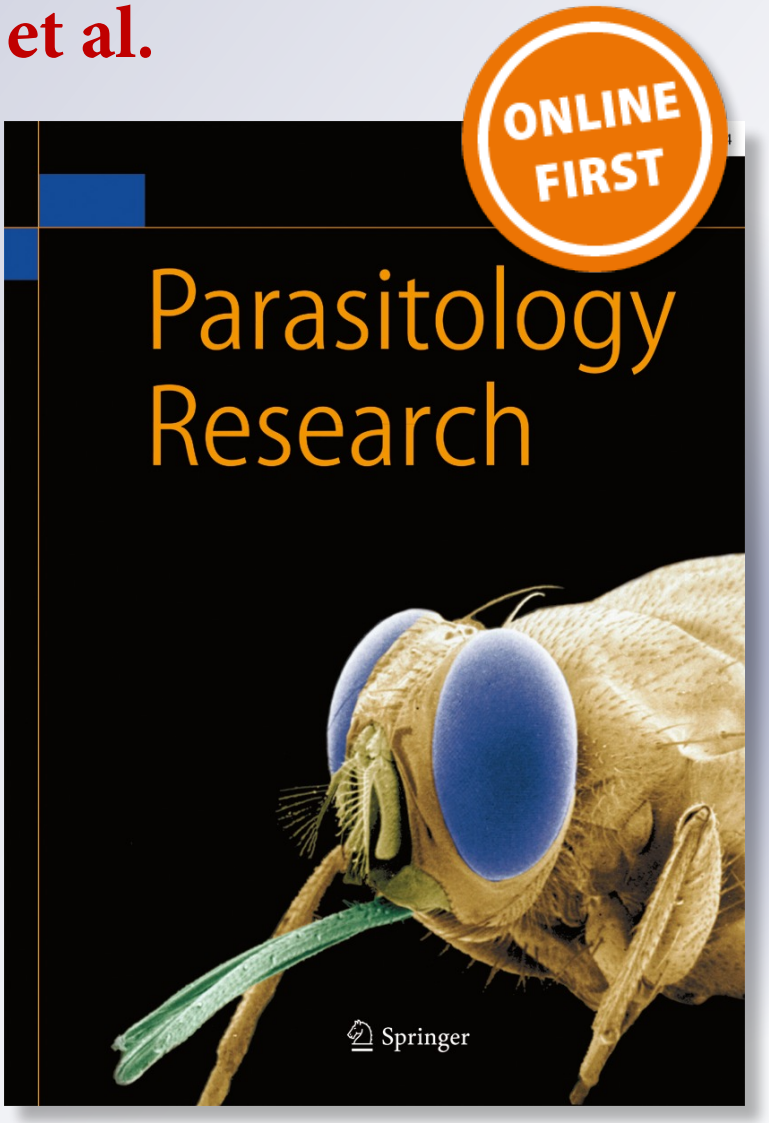

Springer

Parasitol Res
DOI 10.1007/s00436-014-4199-8

ORIGINAL PAPER

Unveiling the effects of berenil, a DNA-binding drug, on *Trypanosoma cruzi*: implications for kDNA ultrastructure and replication

Aline Araujo Zuma · Danielle Pereira Cavalcanti · Marcelo Zogovich · Ana Carolina Loyola Machado · Isabela Cecília Mendes · Marc Thiry · Antonio Galina · Wanderley de Souza · Carlos Renato Machado · Maria Cristina Machado Motta

Received: 14 May 2014 / Accepted: 17 October 2014

Abstract *Trypanosoma cruzi*, the etiological agent of Chagas disease, exhibits a single mitochondrion with an enlarged portion termed kinetoplast. This unique structure harbors the mitochondrial DNA (kDNA), composed of interlocked molecules: minicircles and maxicircles. kDNA is a hallmark of kinetoplastids and for this reason constitutes a valuable target in chemotherapeutic and cell biology studies. In the present work, we analyzed the effects of berenil, a minor-groove-binding agent that acts preferentially at the kDNA, thereby affecting cell proliferation, ultrastructure, and mitochondrial activity of *T. cruzi* epimastigote form. Our results showed that berenil promoted a reduction on parasite growth when high concentrations were used; however, cell viability was not affected. This compound caused significant changes in kDNA arrangement, including the appearance of membrane profiles in the network and electron-lucent areas in the kinetoplast matrix, but nuclear ultrastructure was not modified. The use of the TdT technique, which specifically labels DNA, conjugated to atomic force microscopy analysis indicates that berenil prevents the minicircle decatenation of the network, thus impairing DNA replication and culminating in the appearance of dyskinetoplastic cells. Alterations in the kinetoplast network may be associated with kDNA lesions, as suggested by the quantitative PCR (qPCR) technique. Furthermore, parasites treated with berenil presented higher levels of reactive oxygen species and a slight decrease in the mitochondrial membrane potential and oxygen consumption. Taken together, our results reveal that this DNA-binding drug mainly affects kDNA topology and replication, reinforcing the idea that the kinetoplast represents a potential target for chemotherapy against trypanosomatids.

Keywords DNA-binding drugs · kDNA topology and replication · Kinetoplast · *Trypanosoma cruzi* · Ultrastructure

Electronic supplementary material The online version of this article (doi:10.1007/s00436-014-4199-8) contains supplementary material, which is available to authorized users.

A. A. Zuma · A. C. L. Machado · W. de Souza · M. C. M. Motta
Laboratório de Ultraestrutura Celular Hertha Meyer, Instituto de Biofísica Carlos Chagas Filho, Universidade Federal do Rio de Janeiro, 21491-590 Rio de Janeiro, RJ, Brazil

A. A. Zuma · D. P. Cavalcanti · M. Zogovich · A. C. L. Machado · W. de Souza · M. C. M. Motta (✉)
Instituto Nacional de Metrologia, Qualidade e Tecnologia-Inmetro, 25250-020 Duque de Caxias, RJ, Brazil
e-mail: motta@biof.ufrj.br

I. C. Mendes · C. R. Machado
Laboratório de Genética Bioquímica, Departamento de Bioquímica e Imunologia, Instituto de Ciências Biológicas, Universidade Federal de Minas Gerais, 31270-901 Belo Horizonte, MG, Brazil

M. Thiry
Department of life Sciences, GIGA-Neurosciences, Unit of Cell and Tissue Biology, University of Liege, Liege, Belgium

A. Galina
Laboratório de Bioenergética e Fisiologia Mitocondrial, Programa de Biofísica e Bioquímica Celular, Instituto de Bioquímica Médica Leopoldo de Meis, Universidade Federal do Rio de Janeiro, 21491-590 Rio de Janeiro, RJ, Brazil

Introduction

Trypanosomatids are parasites with a worldwide distribution, and many of them are the etiological agents of endemic diseases to human and animals. In Latin America, Chagas disease, caused by *Trypanosoma cruzi*, affects approximately

Published online: 29 October 2014

8 million people. In Africa, *Trypanosoma brucei* causes sleeping sickness in humans and nagana in animals, whereas species of the *Leishmania* genus cause leishmaniasis in underdeveloped countries (de Souza 2002; Jensen and Englund 2012; Kennedy 2013). In this sense, intensive studies have been performed to develop new chemotherapy compounds and to find exclusive targets in trypanosomatid protozoa.

The Trypanosomatidae family presents remarkable features, such as a single mitochondrion that contains an enlarged region, termed kinetoplast, which harbors the mitochondrial DNA (kDNA). The kDNA presents a unique network composed of interlocked DNA molecules: the minicircles and maxicircles. The minicircles encode guide RNAs that participate in the editing of transcripts produced by the maxicircles, which are responsible for producing rRNAs and proteins of the respiratory chain. During the parasite cell cycle, these circular molecules need to be replicated and then equally segregated between daughter cells. kDNA replication begins when topoisomerase II releases each minicircle from the network to the kinetoflagellar zone (KFZ), where universal minicircle binding protein (UMBSP) recognizes a specific sequence of the ring that corresponds to the replication origin. Then, primases produce the RNA primers required for initiating DNA synthesis, generating minicircles in theta intermediate forms that are reattached to the kinetoplast antipodal sites by topo II. Finally, the primers are removed from the minicircles by the SSE1 enzyme, and the gaps between Okazaki fragments are filled by polymerase β. The nicks are sealed by DNA ligase only when all minicircle replication is completed to guarantee that this event occurs only once in the cell cycle (reviewed by Jensen and Englund 2012).

Because the arrangement and replication of kDNA catenated circles are unique in nature, the kinetoplast may represent a potential target for chemotherapeutic studies and also an interesting structure for a better understanding of the biology of trypanosomatid protozoa. It is also worth considering that the mitochondrion is a symbiont-derived organelle; thus, kDNA presents particular features, such as AT-rich regions, corresponding to approximately 60 % of *T. cruzi* mitochondrial DNA base pairs (Brack et al. 1972a). Such a characteristic prompted us to investigate the effects of compounds that bind to the DNA minor groove and have a high affinity for AT-rich regions (Brack et al. 1972a). These compounds, termed minor groove binders, are natural or synthetic products and include aromatic diamidines, such as pentamidine and berenil (diminazene aceturate) (Brack et al. 1972a; Barrett et al. 2013). Different from intercalating agents such as acriflavine, DNA binders do not insert between two base pairs, present a greater association with DNA, and do not require free energy expenditure during the binding process (Palchaudhuri and Hergenrother 2007).

Berenil has been used in the treatment of domestic livestock trypanosomiasis and babesiosis (Peregrine and Mamman 1993; Barrett et al. 2013). In trypanosomes, this compound inhibits mitochondrial topoisomerase II activity and consequently might interfere with kDNA replication (Shapiro and Englund 1990). The specific binding of berenil to kinetoplast DNA is also supported by the fact that there is no detectable effect on nuclear DNA after treatment with this compound (Macadam and Williamson 1972; Shapiro and Englund 1990).

Several works describe the effects of berenil in *T. brucei* (Egbe-Nwiyi et al. 2003; Egbe-Nwiyi et al. 2005; Witola et al. 2005) or in isolated kDNA (Brack et al. 1972a); however, the mechanism of action of this DNA-binding compound is still unexplored in trypanosomatids. Thus, in this work, we examined the effects of berenil on *T. cruzi* proliferation, mitochondrial activity, DNA damage, and kDNA ultrastructural organization using different approaches. Our results indicate that the kDNA lesions promoted by berenil may induce cell growth inhibition and kDNA rearrangement, thus resulting in the abrogation of minicircle replication and culminating in increases in the number of dyskinetoplastic protozoa. Mitochondrial physiology was also affected because this organelle presented elevated amounts of reactive oxygen species as well as a slight decrease in the membrane potential and in oxygen consumption.

Materials and methods

Protozoa culture

T. cruzi epimastigote forms (Y strain) were cultivated for 24 h at 28 °C in liver infusion tryptose (LIT) medium (Camargo 1964) supplemented with 10 % fetal calf serum.

Drug treatment

Berenil was diluted in Milli-Q water at 5 mM and was added to the culture medium after 24 h of initial growth, which corresponds to the logarithmic phase. The drug concentrations used in this work (2, 10, 20, and 50 μM) were determined according to data presented in previous reports (Portugal 1994; Witola et al. 2005; Zuma et al. 2011).

Transmission electron microscopy

Routine

Parasites were washed in PBS (pH 7.2) and fixed in 2.5 % glutaraldehyde diluted in 0.1-M cacodylate buffer (pH 7.2) at room temperature; after 1 h, they were washed in the same buffer. Cells were postfixed in 0.1-M cacodylate buffer containing 1 % OsO_4 and 0.8 % potassium ferricyanide for 1 h.

The protozoa were then washed in the same buffer, were dehydrated in a graded series of acetone, and embedded in Epon (Electron Microscopy Sciences, Hatfield, PA). Ultrathin sections were stained with uranyl acetate and lead citrate and were observed using a Zeiss 900 transmission electron microscope (Zeiss, Oberkochen, Germany).

Immunocytochemical technique—terminal deoxynucleotidyl transferase

The terminal deoxynucleotidyl transferase (TdT) technique was performed as described by Motta et al. (2003). For this assay, grids containing thin sections were incubated in a solution containing 5′-bromo-2′-deoxyuridine (BrdU), calf thymus TdT, and dNTPs (dCTP, dGTP, and dATP). The thin sections were then incubated with a monoclonal anti-BrdU anti-body, washed, and incubated with goat-anti-mouse IgG coupled to colloidal gold of 10-nm diameter. The samples were stained as in the routine method.

kDNA isolation

kDNA networks were isolated according to the protocol described by Pérez-Morga and Englund (1993). Nontreated and protozoa treated with 20 and 50 μM of berenil for 48 h were harvested by centrifugation and washed in NET 100 buffer (i.e., 10 mM Tris-HCl [pH 8.0], 100 mM NaCl, and 100 mM EDTA). The cells were lysed at 37 °C for 60 min in a solution containing 56.5 μl of 20 % SDS and 11 μl of proteinase K (20 mg/ml) diluted in 1 ml of NET 100 buffer. The lysate was loaded onto a 20 % sucrose cushion and centrifuged for 20 min at 18,000*g* in an Eppendorf 5810R centrifuge. The kDNA pellet was resuspended in NET 100, loaded on top of a second sucrose cushion, and processed as previously described. The kDNA was dialyzed against Tris-EDTA buffer (i.e., 10 mM Tris-HCl [pH 8.0] and 1 mM EDTA) overnight, centrifuged at 18,000×*g* for 30 min, and resuspended in 1 mM Tris-HCl, pH 8.0.

Atomic force microscopy (AFM)

The isolated kDNA networks were prepared for AFM analyses as described by Cavalcanti et al. (2011). Briefly, the solution containing the kDNA networks was mixed with 25 mM magnesium chloride and then deposited onto a freshly cleaved mica surface. The sample was critical point dried in a Leica EM CPD030 apparatus according to the manufacturer's instructions. The network images were acquired with a BioScope Catalyst AFM (Bruker Corporation) using the Tapping mode in air. The AF microscope was mounted with a high-resolution probe (nanotools® MSS-FMR-13) working in a nominal resonant frequency of approximately 70 kHz. The images were processed using the NanoScope analysis software.

Fluorescence microscopy

To asses the occurrence of dyskinetoplasty, parasites were washed in PBS, fixed in 4 % formaldehyde in PBS for 5 min, and washed. The cells were then deposited on slides previously coated with poly-L-lysine for 10 min; the slides were then washed. The cells were incubated with 4′,6-diamidino-2-phenylindole (DAPI, from Molecular Probes) diluted at 1:500 for 5 min. The slides were then washed, mounted in N-propyl gallate, and observed using a Zeiss Axioplan light microscope. To verify the number of dyskinetoplastic parasites, cell counting was achieved based on the presence of kDNA after DAPI staining.

Analysis of DNA lesions using quantitative PCR (qPCR) assay

For this assay, cells were treated with 50 μM for up to 72 h. Parasite cultures containing 1×10^7 cells/ml were harvested by centrifugation at 3,000×*g* for 10 min. The supernatant (conditioned medium) was saved for later use, and the cells were resuspended in PBS. DNA extraction and quantification, QPCR amplification, and analyses were conducted as reported previously (Regis-da-Silva et al. 2006). The qPCR assay compared the amplification of the DNA from a treated sample with the amplification obtained with the untreated control. Specific primers were used to amplify large and small fragments of the nuclear and mitochondrial DNA. The large nuclear fragment was amplified using the forward primer QPCRNuc2F (5′-GCACACGGCTGCGAGTGACCATTCAACTTT-3′) and the reverse primer QPCRNuc2R (5′-CCTCGCACATTTCT ACCTTGTCCTTCAATGCCTGC-3′). The small nuclear fragment was amplified with the internal primer QPCRNuc2Int (5′-tcgagcaagctgacactcgatgcaaccaaag-3′) and the reverse primer QPCRNuc2R. The large mitochondrial fragment was amplified using the forward primer QPCRMitF (5′-TTTTATTTGGGG GAGAACGGAGCG-3′) and the reverse primer QPCRMitR (5′-TTGAAACTGCTTTCCCCAAACGCC-3′). The small mitochondrial fragment was amplified with the internal primer QPCRMitInt (5′-CGCTCTGCCCCCATAAAAAACCTT-3′). Because the probability of introducing a lesion in a short segment is very low, the small fragment (250 bp) was used to normalize the amplification results obtained with the large fragments (10 kb). This step eliminates the bias of changes in the proportion between the nuclear and mitochondrial genomes. All of the primer sets were amplified in a specific

manner, i.e., they produced only one band, as verified by gel electrophoresis (data not show). The normalized amplification of the treated samples was then compared with the controls, and the relative amplification was calculated. These values were used to estimate the average number of lesions per 10 kb of genome through a Poisson distribution. The final results are the mean of two sets of qPCR results for each target gene from at least two biological experiments.

Determination of mitochondrial membrane potential ($\Delta\Psi m$)

Protozoa were washed with PBS (pH 7.2) and then added to a reaction medium (125 mM sucrose, 65 mM KCl, 10 mM HEPES/K^+ pH 7.2, 2 mM Pi, 1 mM $MgCl_2$, and 500 μM EGTA). Approximately 1×10^7 cells were incubated in 10 μg/ml JC-1 (a probe used to detect loss of $\Delta\Psi m$), and the absorbance was measured at every minute for 30 min using a microplate reader (Macedo-Silva et al. 2011). We also used 1 μM FCCP (a protonophore used to dissipate proton gradients) as a positive control for the depolarization of $\Delta\Psi m$ and 2 μM of FCCP at the end of the measurement to fully decrease $\Delta\Psi m$.

Measurement of O_2 consumption

Cells were washed in PBS (pH 7.2), and 10^8 parasites were incubated in a reaction medium (125 mM sucrose, 65 mM KCl, 2 mM KH2PO4, 0.5 mM $MgCl_2$, 10 mM HEPES pH 7.2, 1 mM EGTA, and 1 mg/ml BSA) (Silva et al. 2011). The analysis was performed using high-resolution respirometry with the OROBOROS Oxygraph-2 k. After oxygen uptake stabilization, the cells were permeabilized with 15 μM digitonin, and the substrates 5 mM succinate and 200 μM ADP were added to the medium. At the end of the experiment, 1 mM KCN was added to inhibit oxygen consumption.

Measurement of reactive oxygen species (ROS) production

Parasites (approximately 2.5×107) were incubated in 10 μg/ml H2DCFDA in PBS, pH 7.2, for 1 h at 28 °C. H2DCFDA is a nonfluorescent dye that becomes fluorescent in the presence of ROS. As a positive control for ROS production, we used 10 μM oligomycin. The cells were analyzed using a microplate reader, and ROS levels were measured using the wavelengths of 507 nm as emission and 530 nm as excitation.

Cell viability

Cell viability was examined using the MTS/PMS method (Henriques et al. 2011). In viable cells, the reagent PMS is reduced, and the electrons are transferred to MTS, which is converted by dehydrogenase enzymes into a water-soluble compound, formazan, in proportion to the number of viable cells. Parasites were incubated with MTS/PMS solution for 4 h. As a negative control, parasites were fixed with 0.4 % formaldehyde for 10 min at room temperature. The cells were analyzed using a spectrofluorometer (Molecular Devices Microplate Reader (SpectraMax M2/M2e, Molecular Devices) at 490 nm.

Results

Berenil caused a significant reduction on *T. cruzi* proliferation after treatment with 20 μM for 48 and 72 h, which is equivalent to 39 and 42 %, respectively. This reduction was more pronounced after treatment with 50 μM for 72 h, which reached 58 % of inhibition compared to control cells. Treatment with lower concentrations of berenil did not considerably affect cell proliferation (Fig. 1). Such an effect, as previously reported by Zuma et al. (2011), may be related to the fact that this drug promotes remarkable modifications on kinetoplast DNA arrangement, but does not impair cell division. The control cells presented a typical organization, such as a nucleus containing condensed heterochromatin, one mitochondrion, a bar-shaped kinetoplast, a Golgi complex, and a flagellum (Fig. 2a). The parasites treated with 10 μM for 72 h presented an intense mitochondrial swelling with loss of matrix, and many cells lost the typical bar-shaped kDNA. In addition, an electron-dense round point situated in the kinetoplast antipodal site was observed (Fig. 2b). When the

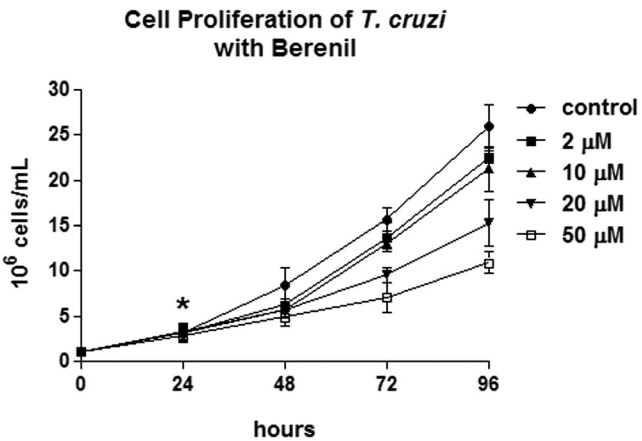

Fig. 1 Proliferation of *Trypanosoma cruzi* epimastigote form after treatment with berenil. The highest inhibition of parasite proliferation was observed 50 μM for 72 h, equivalent to 58 % compared to control cells. The *asterisk* indicates the addition of berenil to the culture medium. The data are the average of three independent experiments

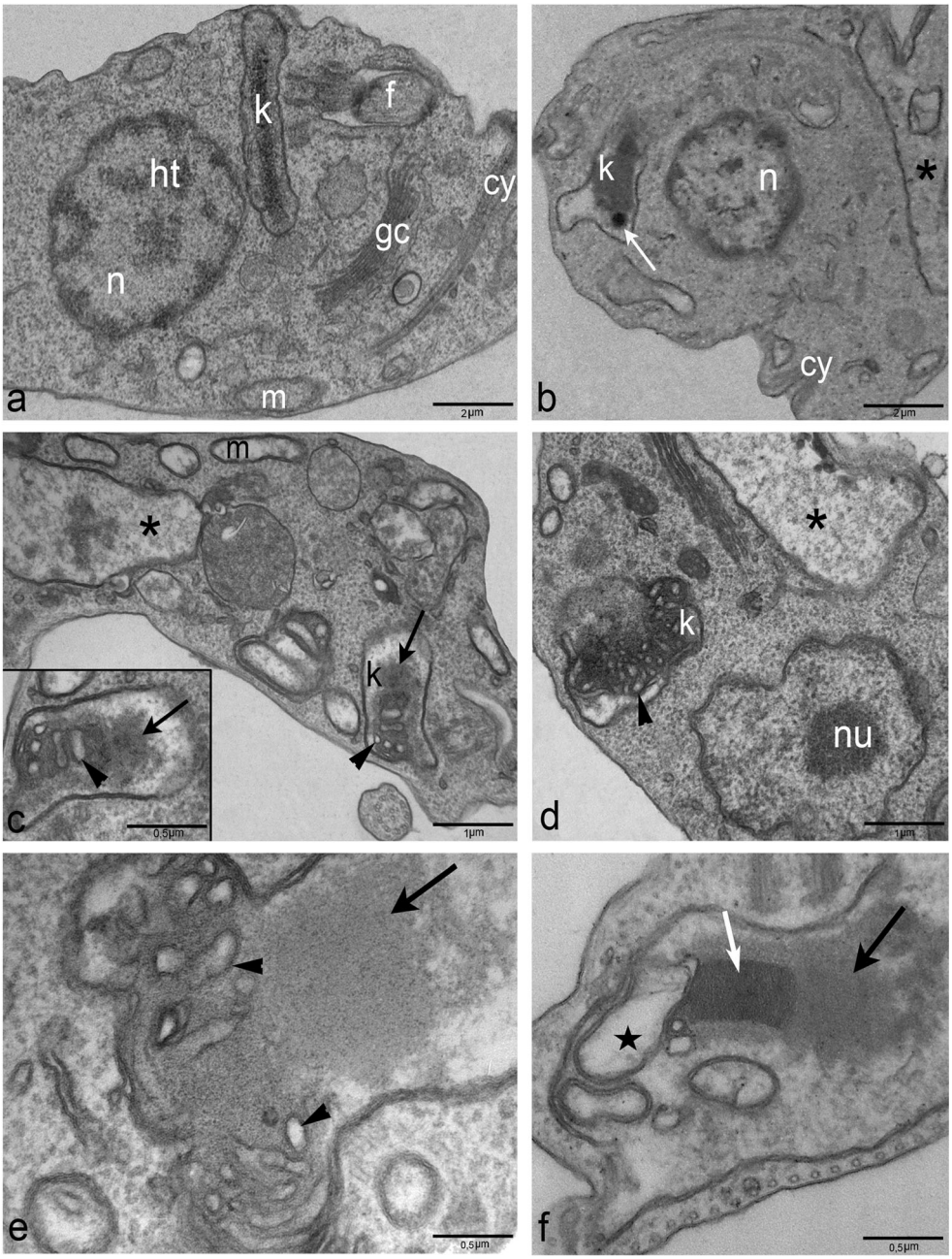

Fig. 2 Transmission electron microscopy of *T. cruzi* epimastigote treated with berenil. **a** Nontreated parasites, showing the nucleus (n), the condensed heterochromatin (ht), the mitochondrion (m), the kinetoplast (k), the Golgi complex (gc), the flagellum (f), and the cystostome (cy). **b** Parasites treated with 10 μM for 72 h. Note the mitochondrial swelling (*asterisk*) and the presence of an electron-dense point situated in the antipodal site (*white arrow*). **c**, **d** *T. cruzi* treated with 20 and 50 μM for 48 h, respectively. Cells presented mitochondrial swelling (*asterisk*), electron-lucid areas near the network (*arrow*), and membrane profiles in the middle of the kDNA (*arrowhead*). *Inset* shows these effects at higher magnification. **e**, **f** Parasites treated with 50 μM for 72 h, showing electron-lucid areas near the network (*arrow*), membrane profiles (*arrowhead*), and enlarged mitochondrial cristae (*star*). Note that part of the kDNA maintains its normal arrangement (*white arrow*)

parasites were treated with 20 μM for 48 h, electron-lucid areas near the kDNA were observed, as was mitochondrial swelling. Interestingly, some cells presented membrane profiles in the middle of the kDNA, which may correspond to invaginations of the inner mitochondrial membrane (Fig. 2c). The same effect occurred after treatment with 50 μM for 48 h, with the membrane invaginations being more pronounced. Despite the kinetoplast alterations, the nuclear ultrastructure was not affected by berenil (Fig. 2d). After treatment with 50 μM for 72 h, we noted a strong kDNA network disorganization and the presence of enlarged mitochondrial cristae in the kinetoplast (Fig. 2e, f).

The electron-lucent areas in the kinetoplast observed by transmission electron microscopy could represent sites of kDNA unpacking caused by the decatenation of the maxicircles and minicircles that compose the network. To understand this kDNA disorganization, we performed the TdT assay, which precisely indicates the location of DNA. In control cells, TdT labeling was observed throughout the nuclear heterochromatin and the kinetoplast, specifically the kDNA and KFZ region (Fig. 3a). However, in the kinetoplast of parasites treated with 20 and 50 μM for 48 h, the gold-particle distribution was restricted to the more condensed areas, whereas the electron-lucent sites were not

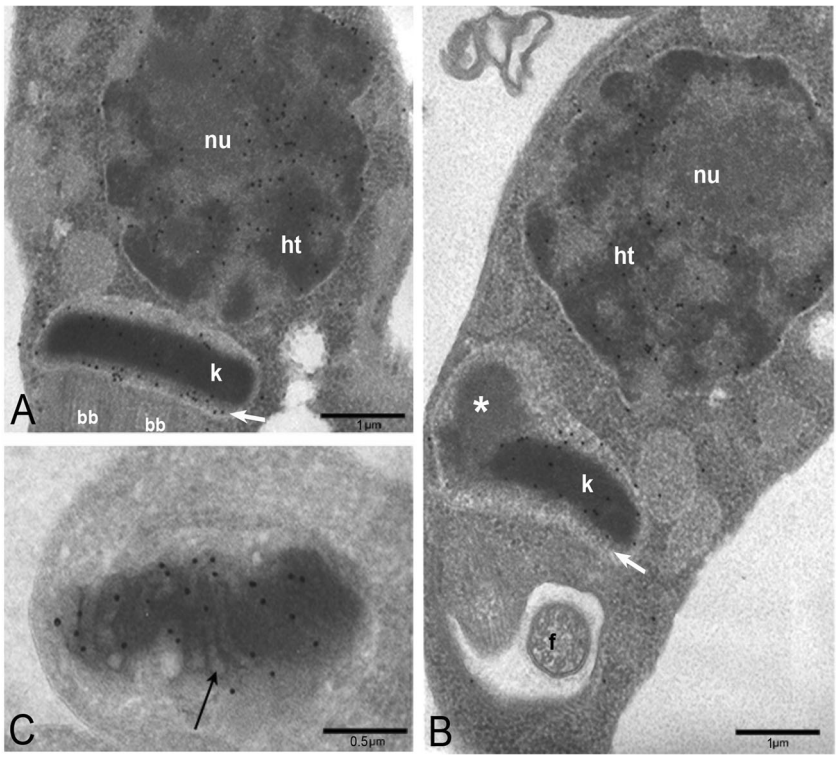

Fig. 3 DNA localization after treatment with berenil, using the TdT technique. **a** Control cells showing the distribution of gold particles in the kinetoplast (k) and the nuclear heterochromatin (ht). Note that the KFZ region (*white arrow*) is labeled by gold particles indicating the presence of replication minicircles. *nu* nucleolus, *bb* basal body. **b** *T. cruzi* treated with 20 μM for 48 h. Note that labeling was observed in the more condensed region of the network (k), but not in the electron-lucent area (*asterisks*). Interestingly, the KFZ region (*white arrow*) is devoid of gold particles. *F* flagellum. **c** *T. cruzi* with 50 μM for 72 h. *The black arrow* indicates a region containing membrane profiles in the kDNA

immunolabeled, indicating that this region did not contain DNA. Interestingly, the KFZ region was not labeled, indicating the absence of free-replicating minicircles in this kinetoplast area (Fig. 3b–d).

To better understand how berenil promotes alterations in the kDNA arrangement, we isolated intact networks of treated and nontreated protozoa and analyzed the samples using AFM. In the nontreated parasites, the isolated kDNA appeared as an intact and massive network, presenting its typical arrangement with fibers homogeneously distributed throughout the network (Fig. 4a, b). In the cells treated with 20 μM berenil for 48 h, the organization of most networks was similar to the control. However, several protozoa presented a more compact arrangement of the kDNA in the central area of the network (Fig. 4c, d—arrow). After treatment with 50 μM for 48 h, the effect of berenil on kDNA organization was more intense, and condensed kDNA regions were also observed at the periphery of the network (Fig. 4e, f—arrow).

Considering that the ultrastructural analyses showed strong alterations in kDNA arrangement, we decided to verify the occurrence of dyskinetoplastic protozoa (DK) in the group of berenil-treated cells. For this purpose, the parasite morphology and presence of kDNA were investigated using fluorescence microscopy. Control cells presented a typical elongated shape of the epimastigote form, which contains a bar-shaped kinetoplast (Fig. 5a). When the parasites were treated with 50 μM berenil for 72 h, the kinetoplast appeared smaller and rounded (Fig. 5b). Furthermore, dividing parasites presented atypical cellular patterns with two nuclei and a single bar-shaped kinetoplast (Fig. 5c) or a rounded format (Fig. 5d), indicating the formation of DK daughter cells after cytokinesis (Fig. 5e). Such parasites are characterized by the partial or total loss of kDNA.

Based on DAPI staining, a quantitative analysis of berenil-treated parasites was performed to determine the percent of dyskinetoplastic cells generated. After treatment with 50 μM for 24 h, only 4 % of the parasites were dyskinetoplastic. However, after 48 h of cell exposure to this DNA binder, this percentage increased significantly to 33 and to 37 % after 72 h (Fig. 6).

Due to the striking disorganization that berenil caused in kDNA arrangement, we performed qPCR to determine whether there were lesions in the kinetoplast and in the nuclear DNA. The number of kDNA lesions in the parasites treated with 50 μM increased as the treatment proceeded, reaching approximately 1 lesion per 10 kb of DNA after 72 h. However, no lesions were detected in the nuclear DNA (Fig. 7), which is in accordance with the results obtained by electron microscopy.

According to our ultrastructural analyses, the mitochondrion was the most altered organelle after treatment with berenil. Thus, to investigate whether mitochondrial function was affected, the membrane potential, the consumption of oxygen, and the generation of ROS were analyzed. The results showed that the mitochondrial membrane potential did not decrease when the cells were exposed to 2 μM berenil for 72 h. However, this value started to decline after treatment with 10 μM, decreasing by 20 %. After treatment with 20 and

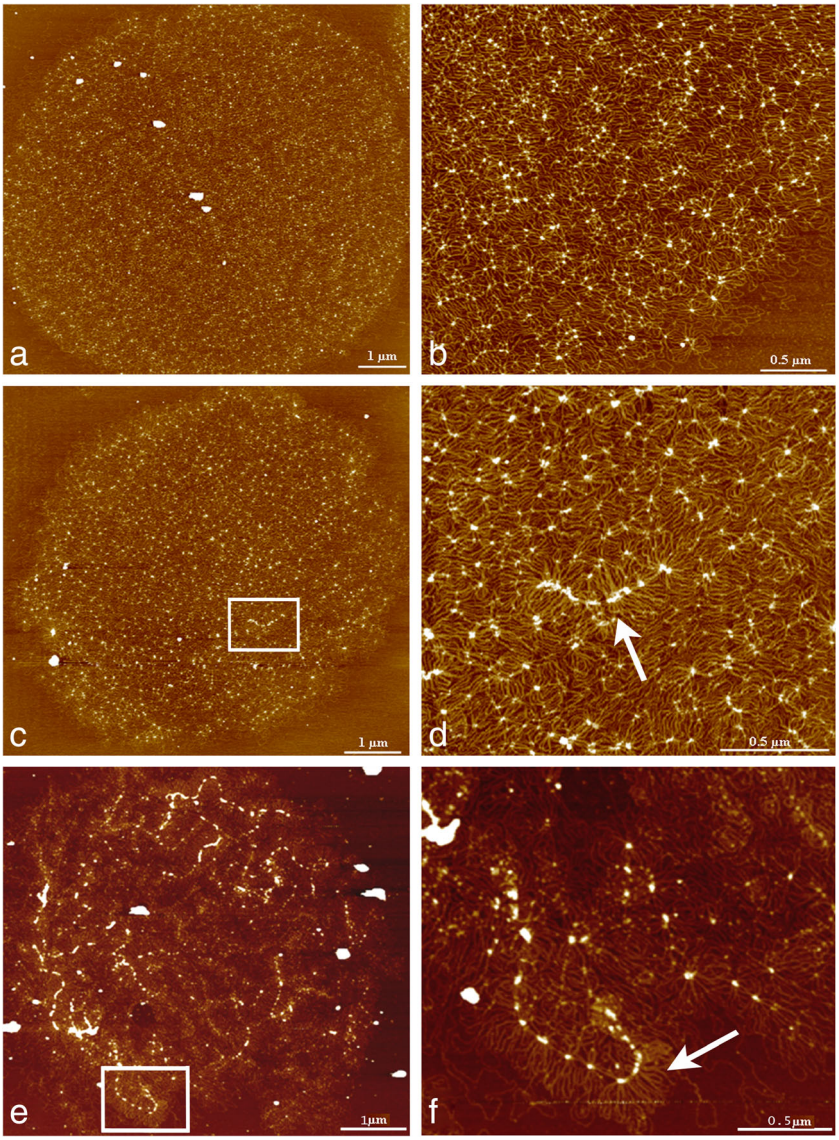

Fig. 4 Atomic force microscopy (AFM) of isolated kDNA obtained from *T. cruzi* epimastigotes treated with berenil. **a**, **b** An intact network of nontreated parasites. In **b**, the enlargement permits to observe the homogeneous distribution of minicircles throughout the network. **c**, **d** kDNA of *T. cruzi* treated with 20 μM berenil for 48 h. *The square* in **c** was enlarged as observed in **d** and permits the observation of condensed areas of kDNA in the middle of the network (*arrow*). **e**, **f** kDNA of *T. cruzi* treated with 50 μM for 48 h. It is possible to note a complete disorganization of the kDNA. *The square* in **e** was enlarged as observed in **f**, revealing a more compact region in the periphery of the network (*arrow*)

50 μM berenil, the arbitrary unit of JC1 (ΔΨm) was 33 % lower when compared to the control parasites (Fig. 8a). Considering the O_2 consumption of intact cells, we observed that treatment with the highest concentration (50 μM) of berenil for 72 h slightly decreased O_2 consumption in approximately 17 % of the treated cells when compared to control cells (Fig. 8b). KCN, a specific inhibitor of cytochrome oxidase, was added at the end of the assays as a negative control (Fig. 8b). Moreover, the titration of succinate and ADP slightly reduced the O2 uptake rate (data not shown). ROS generation in the parasites treated with 2 and 10 μM berenil for 72 h was very similar to the control group. However, in the parasites treated with 20 and 50 μM for the same period, the levels of ROS were 2 and 3 times higher, respectively, when compared to the nontreated parasites (Fig. 8c). According to the viability test, which considered mitochondrion functioning, most cells remained viable (90 %) even after treatment with 50 μM for 72 h (Fig. 8d), although cell proliferation was reduced in such conditions.

Discussion

DNA-binding drugs such as berenil comprise a class of inhibitors that binds to the DNA minor groove leading to topological modifications and consequently interfering with topoisomerase activity. Because this compound presents high affinity for AT-rich regions, it preferentially binds to kinetoplast DNA and interferes indirectly with topoisomerase II activity (Wilson et al. 2005). The effect of inhibitors that promote modifications in kDNA arrangement and replication has been described, reinforcing the idea that the kinetoplast constitutes an important target in chemotherapeutic studies involving trypanosomatid protozoa (Brack et al. 1972a; Portugal 1994; Liu et al. 2005).

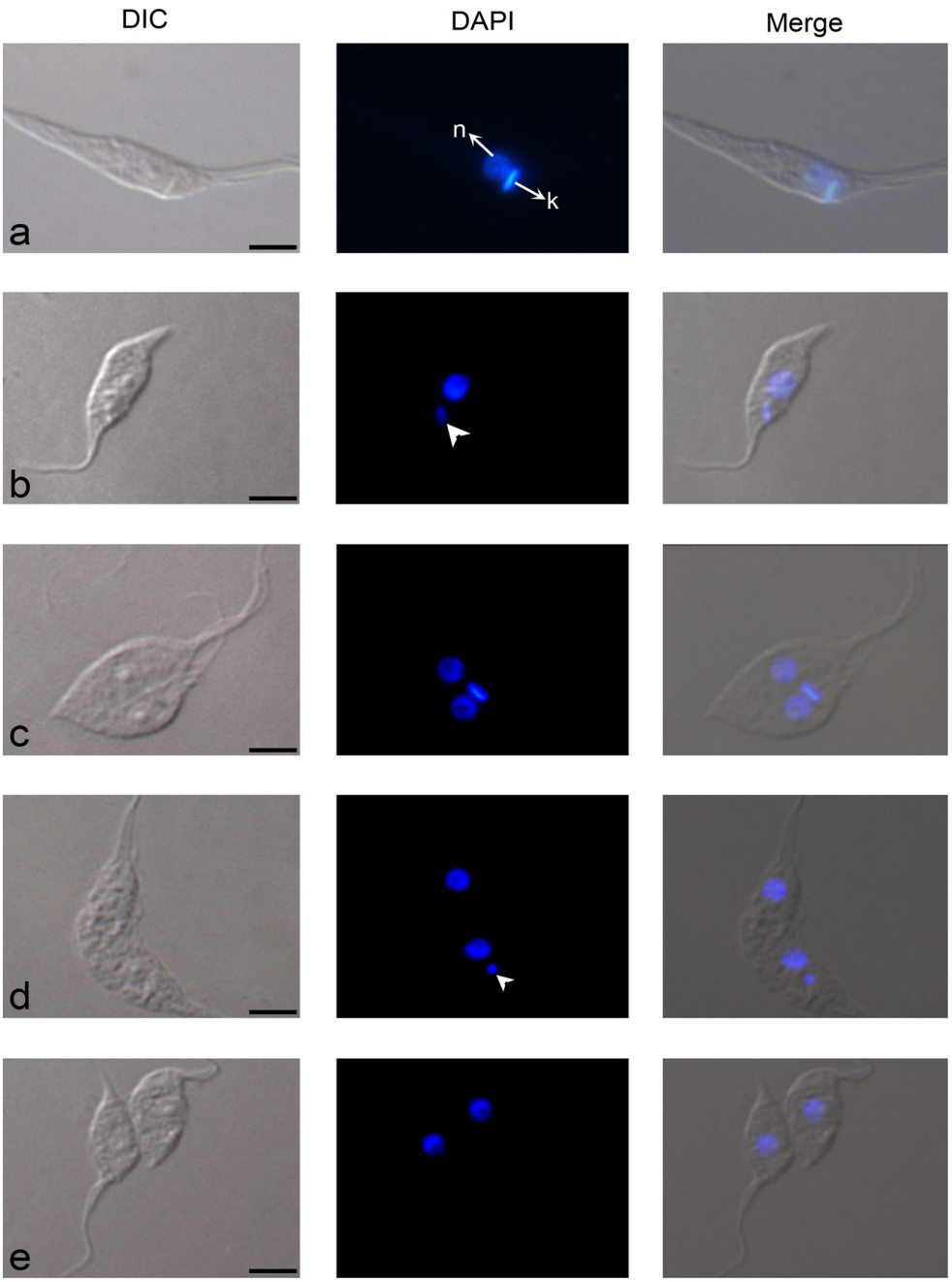

Fig. 5 Fluorescence optical microscopy of *T. cruzi* treated with berenil using DAPI to label nucleus and kinetoplast. **a** Control parasites showing the nucleus (n) and the bar shape kinetoplast (k). **b**–**e** Parasites treated with 50 μM for 72 h. **b** Note that the kDNA was rounded (*arrowhead*). **c**, **d** During cytokinesis, atypical cellular patterns were observed containing two nuclei and a single kinetoplast, resulting in the appearance of dyskinetoplastic parasites (**e**)

T. cruzi epimastigote proliferation was only affected when high concentrations of berenil (20 and 50 μM) were used for 48 h of treatment; however, such conditions did not reduce cell viability. The main effect of berenil was observed on kinetoplast, which presented alteration on kDNA arrangement; however, the nuclear ultrastructure was not modified. In this work, a more profound structural analysis using transmission electron microscopy revealed that the kDNA disorganization is related to the appearance of electron-lucid areas in the kinetoplast matrix, membrane profiles in the middle of the network, and an electron-dense point in the antipodal site region.

Diamidines are minor groove binders well known for their antiparasitic potential. These compounds have been tested successfully against *T. cruzi* bloodstream trypomastigotes (de Souza et al. 2011) and against *L. donovani* (Wang et al. 2010), thus representing alternative drugs for trypanosomiasis treatments. Diamidines promote ultrastructural modifications in *T. cruzi* amastigotes that are similar to those described in this work, especially mitochondrial swelling and kDNA disorganization (Silva et al. 2007). However, the membrane profiles here reported in the middle of the kDNA network were not observed in the intracellular form. Trypomastigotes present distinct kDNA ultrastructural effects after diamidine

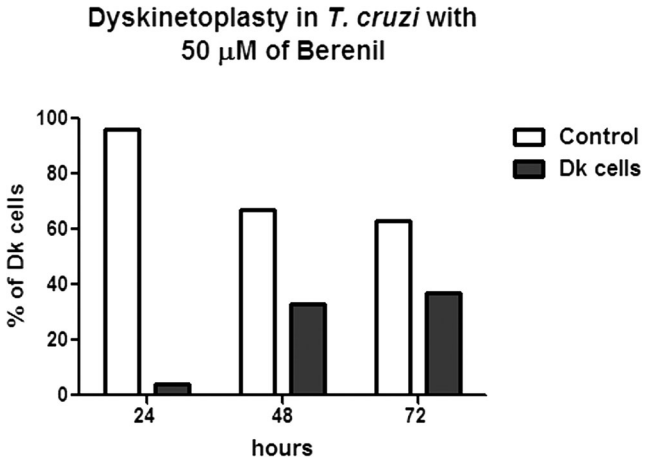

Fig. 6 Quantification of dyskinetoplastic (DK) parasites after treatment with berenil. The percentage of DK cells significantly increased after 48 h of treatment and reached 37 % after 72 h

treatment, and this is most likely related to the looser kDNA arrangement (Silva et al. 2007). Although the effects of diamidines were described on parasite kDNA ultrastructure, there are no reports about alterations in the mitochondrial DNA of host cells.

To better understand the ultrastructural modifications after treatment with berenil, we used the TdT technique, which specifically labels DNA and was previously employed to study the *T. cruzi* cell cycle (Elias et al. 2002). Our results showed that the kinetoplast electron-lucent areas observed in treated parasites were not labeled, thus indicating that this region did not contain decatenated circles, as initially thought. Interestingly, the KFZ region was labeled only in the control cells, and not in the treated cells, suggesting that somehow, the topological alterations suffered by the kDNA after berenil

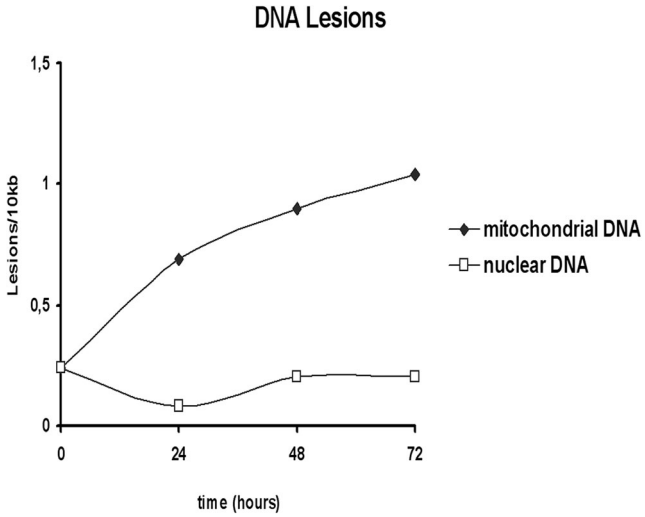

Fig. 7 Quantitative qPCR-based measurement of berenil-induced lesions after treatment with 50 μM up to 72 h. Detection of one lesion per 10 kb of DNA was observed in the mitochondrial DNA. In the nuclear DNA, no lesions were detected

treatment abrogated the release of minicircles from the network. In accordance with this idea, the AFM technique showed that berenil promoted kDNA compaction in the central and peripheral regions of the network. Alterations in *T. cruzi* kDNA organization after berenil treatment were also proposed by Brack et al. (1972b), who reported kinetoplasts presenting densely packed minicircles, especially in the network periphery. It is also worth mentioning that detached circles were not observed as previously reported in *T. cruzi* treated with acriflavine, an intercalating agent (Manchester et al. 2013). Our data obtained by AFM are also consistent with those published by Portugal (1994) showing that berenil prevented minicircle release, thus suggesting the impairment of kDNA replication.

According to Trager and Rudzinska (1964), parasites are considered dyskinetoplastic (DK) when Giemsa staining of the kinetoplast is no longer detectable and the kDNA appears altered by transmission electron microscopy. In the present work, we suggest that the ultrastructural alterations of kDNA promoted by berenil are related to cell growth inhibition and minicircle replication impairment, which culminate in the generation of DK parasites. The occurrence of DK cells has been described in *Leishmania tarentolae*, *Crithidia fasciculata*, *T. brucei*, *T. equiperdum*, and *T. cruzi* treated with acriflavine (Simpson 1968; Hill and Anderson 1969; Stuart 1971; Hajduk 1979; Manchester et al. 2013). These works also reported a size reduction of the kinetoplast and the maintenance of the nuclear structure, as we also observed in *T. cruzi* treated with berenil. It is worth discussing that groove-binding drugs and intercalating agents most likely cause dyskinetoplasty via different mechanisms of action: For example, berenil prevents minicircle release from the network, whereas acriflavine promotes minicircle detachment (Manchester et al. 2013). However, in both cases, kDNA replication is impaired, generating DK cells. It is worth mentioning that some trypanosomatid species do not present kDNA and are naturally dyskinetoplastic. Although the typical kinetoplast is absent in these protozoa, they are viable because their energetic metabolism does not depend exclusively on mitochondrial respiration.

Nonetheless, despite all the ultrastructural alterations promoted by berenil in the kinetoplast of *T. cruzi*, there was no indication of cell cycle arrest. This suggests that the prevention of mitochondrial DNA replication was not able to promote cell cycle blockade, as observed when nuclear DNA is affected by camptothecin, a topoisomerase I inhibitor that promotes heterochromatin unpacking (Zuma et al. 2014).

In agreement with microscopy analyses, our qPCR assays showed that berenil caused damage to the kDNA, but not the nuclear DNA, which can be affected after treatment with camptothecin (Zuma et al. 2014). These data reinforce the idea that the kinetoplast is the main target of berenil (Macadam and Williamson 1972; Shapiro and Englund 1990). In fact, the mitochondrion as a whole was the most affected organelle in

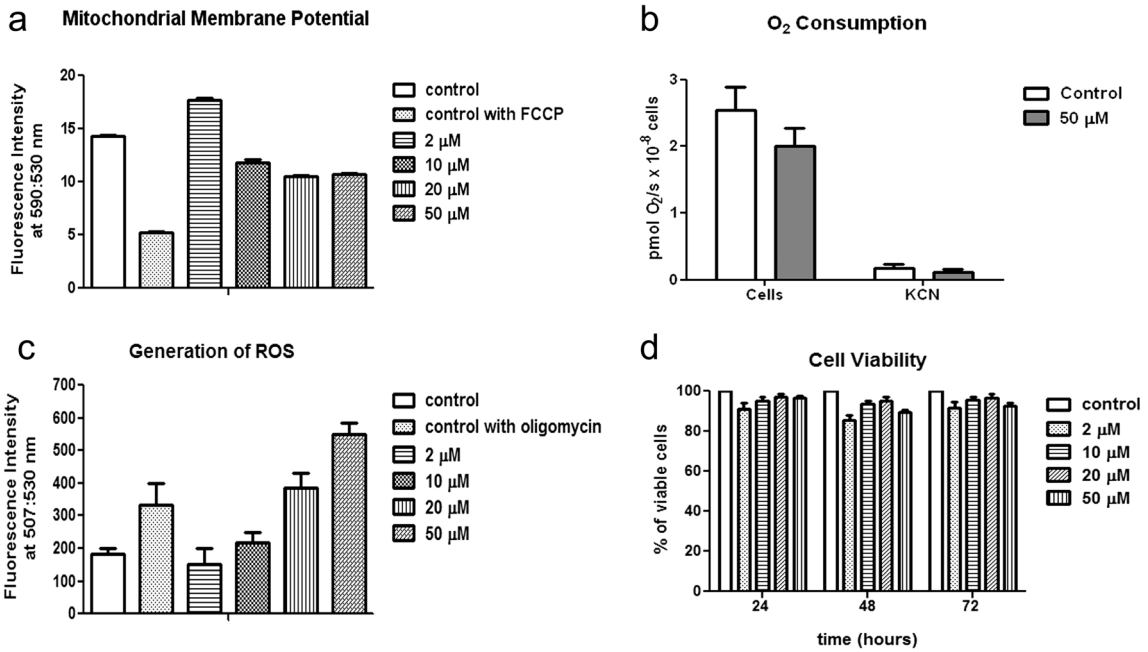

Fig. 8 Analysis of mitochondrial activity in *T. cruzi* treated with berenil for 72 h. **a** The analysis of the mitochondrial membrane potential indicated a potential reduction after treatment with 10 μM. **b** The O_2 consumption presented a significant decrease after treatment with 50 μM. **c** The ROS production augmented in treated parasites in a concentration-dependent manner. **d** *T. cruzi* viability was not significantly reduced by berenil treatment. The data are the average of three independent experiments

T. cruzi after berenil treatment, as revealed by different methodologies that assessed mitochondrial physiology. An evaluation of the membrane potential (ΔΨm) clearly showed that the cells treated with 10 μM for 72 h have an altered ion concentration gradient between the matrix and intermembrane space, which resulted in a decrease in ΔΨm compared to the control cells. Protozoa treatment with 20 and 50 μM of berenil was more drastic, because the decrease in ΔΨm started immediately after addition of the drug. Alterations in the mitochondrial membrane potential are directly related to the production of ROS (Korshunov et al. 1997). In this sense, the berenil-treated protozoa presented increased ROS generation, which duplicated or triplicated after exposure to 20 or 50 μM of the drug, respectively, for 72 h when compared to the control cells. It is noteworthy that ROS production was enhanced as the treatment proceeded from 24 to 72 h using different drug concentrations, especially 20 and 50 μM (Online Resource 1).

As previously reported, the production of ROS may be related to lesions in mitochondrial and nuclear DNA (Storr et al. 2013). Thus, we can suggest that the lesions detected in *T. cruzi* kDNA by qPCR after treatment with berenil may have been caused by ROS and are not only a result of the ultrastructural alterations promoted by this DNA-binding drug. In addition, O_2 consumption was slightly reduced after berenil treatment. These data indicate that berenil induced mitochondrial ROS generation in addition to causing changes in mitochondrial functioning; however, the specific mechanism of alteration in the imbalance of ROS metabolism deserves further investigation. Because these assays were performed in the presence of KCN, our data indicate that most of the O_2 uptake was associated with oxidative phosphorylation and not an alternative oxidase enzyme. It is important to note that despite all these important alterations in mitochondrial physiology, the O_2 consumption slightly decayed indicating that the organelle functioning was preserved, permitting that treated parasites remained viable even after 72 h of treatment.

Taking together all the data obtained in the present work, we can propose the berenil mechanism of action in the *T. cruzi* epimastigote form. This minor groove binder selectively targets the kinetoplast and promotes drastic ultrastructural changes in kDNA, which prevents minicircle release from the network and its replication. This reduces parasite proliferation but does not affect its viability, thus enabling cell division and generation of DK cells. Berenil may also promote lesions in kDNA and affect mitochondrial physiology. Because the kinetoplast is unique in nature for presenting a DNA organization and replication completely different from that observed in the mitochondria of other organisms, this structure represents a promising target in the development of new compounds against pathogenic trypanosomatids.

Acknowledgments The authors are grateful to Rachel Rachid, Camila Silva Gonçalves, and Daniela Leão Gonçalves for technical assistance. This work was supported by Fundação Carlos Chagas Filho de Amparo à Pesquisa do Estado do Rio de Janeiro (FAPERJ), Conselho Nacional de Desenvolvimento Científico e Tecnológico (CNPq), and Programa de Apoios a Núcleos de Excelência (Pronex).

Ethical standards Ethical approval was not required in this work.

Conflict of interest We do not have conflict of interest to declare in this work.

References

Barrett MP, Gemmell CG, Suckling CJ (2013) Minor groove binders as anti-infective agents. Pharmacol Ther 139:12–23. doi:10.1016/j.pharmthera.2013.03.002

Brack CH, Delain E, Riou G (1972a) Replicating, covalently, closed, circular DNA from kinetoplasts of *T. cruzi*. Proc Natl Acad Sci 69:1642–1646

Brack CH, Delain E, Riou G, Festy B (1972b) Molecular organization of the kinetoplast DNA of *Trypanosoma cruzi* treated with berenil, a DNA interacting drug. J Ultrastruct Res 39:568–579. doi:10.1016/S0022-5320(72)90122-0

Camargo EP (1964) Growth and differentiation in *Trypanosoma cruzi* I. Origin of metacyclic trypanosomes in liquid media. Rev Inst Med Trop 6:93–100

Cavalcanti DP, Gonçalves DL, Costa LT, De Souza W (2011) The structure of the kinetoplast DNA network of *Crithidia fasciculata* revealed by atomic force microscopy. Micron 42:553–559. doi:10.1016/j.micron.2011.01.009

De Souza W (2002) Special organelles of some pathogenic protozoa. Parasitol Res 88:1013–1025. doi:10.1007/s00136-002-0696-2

De Souza EM, da Silva PB, Nefertiti ASG, Ismail MA, Arafa RK, Tao B, Nixon-Smith CK, Boykin DW, Soeiro MNC (2011) Trypanocidal activity and selectivity in vitro of aromatic amidine compounds upon bloodstream and intracellular forms of *Trypanosoma cruzi*. Exp Parasitol 127:429–435. doi:10.1016/j.exppara.2010.10.010

Egbe-Nwiyi TN, Igbokwe IO, Onyeyili PA (2003) The pathogenicity of diminazene aceturate-resistant *T. brucei* in rats after treatment with the drug. J Comp Pathol 128:188–191. doi:10.1053/jcpa.2002.0599

Egbe-Nwiyi TN, Igbokwe IO, Onyeyili PA (2005) Diminazene aceturate resistence on the virulence of *T. brucei* for rats. J Comp Pathol 133:286–288. doi:10.1016/j.jcpa.2005.05.002

Elias MCQB, Faria M, Mortara RA, Motta MCM, De Souza W, Thiry M, Schenkman S (2002) Chromosome localization changes in the *Trypanosoma cruzi* nucleus. Eukaryot Cell 1:944–953. doi:10.1128/EC.1.6.944-953.2002

Hajduk SL (1979) Dyskinetoplasty in two species of trypanosomatids. J Cell Sci 35:185–202

Henriques C, Moreira TLB, Maia-Brigagão C, Henriques-Pons A, Carvalho TMU, De Souza W (2011) Tetrazolium salt based methods for high-throughput evaluation of anti-parasite chemotherapy. Anal Methods 3:2148–2155. doi:10.1039/C1AY05219E

Hill GC, Anderson WA (1969) Effects of acriflavine on the mitochondria and kinetoplast of *Crithidia fasciculata*. J Cell Biol 41:547–561

Jensen RE, Englund PT (2012) Network news: the replication of kinetoplast DNA. Annu Rev Microbiol 66:473–491. doi:10.1146/annurev-micro-092611-150057

Kennedy PGE (2013) Clinical features, diagnosis, and treatment of human African trypanosomiasis (sleeping sickness). Lancet Neurol 12:186–194. doi:10.1016/S1474-4422(12)70296-X

Korshunov SS, Skulachev VP, Starkov AA (1997) High protonic potential actuates a mechanism of production of reactive oxygen species in mitochondria. FEBS Lett 416:15–18. doi:10.1016/S0014-5793(97)01159-9

LIU B, LIU Y, MOTYKA SA, AGBO EEC, ENGLUND PT (2005) Fellowship of the rings: the replication of kinetoplast DNA. Trends Parasitol 21:363–369. doi:10.1016/j.pt.2005.06.008

Macadam RF, Williamson J (1972) Drug effects on the fine structure of *Trypanosoma rhodesiense*: diamidines. Trans R Soc Trop Med Hyg 66:897–904. doi:10.1016/0035-9203(72)90125-3

Macedo-Silva ST, Silva TLAO, Urbina JA, de Souza W, Rodrigues JCF (2011) Antiproliferative, ultrastructural and physiological effects of amiodarone on promastigote and amastigote forms of *Leishmania amazonensis*. Mol Biol Int 13:876021. doi:10.4061/2011/876021

Manchester TM, Cavalcanti DP, Zogovich M, de Souza W, Motta MCM (2013) Acriflavine treatment promotes dyskinetoplasty in *Trypanosoma cruzi* as revealed by ultrastructural analysis. Parasitology 140:1422–1431. doi:10.1017/S0031182013001029

Motta MC, de Souza W, Thiry M (2003) Immunocytochemical detection of DNA and RNA in endosymbiont-bearing trypanosomatids. FEMS Microbiol Lett 111:17–23

Palchaudhuri R, Hergenrother PJ (2007) DNA as a target for anticancer compounds: methods to determine the mode of binding and the mechanism of action. Curr Opin Biotechnol 18:497–503. doi:10.1016/j.copbio.2007.09.006

Peregrine AS, Mamman M (1993) Pharmacology of diminazene: a review. Acta Trop 54:185–203. doi:10.1016/0001-706X(93)90092-P

Pérez-Morga DL, Englund PT (1993) The structure of replicating kinetoplast DNA networks. J Cell Biol 123:1069–1079

Portugal J (1994) Berenil acts as a poison of eukaryotic topoisomerase II. FEBS Lett 344:136–138. doi:10.1016/0014-5793(94)00363-7

Regis-da-Silva CG, Freitas JM, Passos-Silva DG, Furtado C, Augusto-Pinto L, Pereira MT et al (2006) Characterization of the *Trypanosoma cruzi* Rad51 gene and its role in recombination events associated with the parasite resistance to ionizing radiation. Mol Biochem Parasitol 2:191–200. doi:10.1016/j.molbiopara.2006.05.012

Shapiro TA, Englund PT (1990) Selective cleavage of kinetoplast DNA minicircles promoted by antitrypanosomal drugs. Proc Natl Acad Sci 87:950–954

Silva CF, Meuser MB, De Souza EM, Meirelles MNL, Stephens CE, Som P, Boykin DW, Soeiro MNC (2007) Cellular effects of reversed amidines on *Trypanosoma cruzi*. Antimicrob Agents Chemother 51:3803–3809. doi:10.1128/AAC. 00047-07

Silva TM, Peloso EF, Vitor SC, Ribeiro LH, Gadelha FR (2011) O_2 consumption rates along the growth curve: new insights into *Trypanosoma cruzi* mitochondrial respiratory chain. J Bioenerg Biomembr 43:409–417. doi:10.1007/s10863-011-9369-0

Simpson L (1968) Effect of acriflavine on the kinetoplast of *L. tarentolae*. Mode of action and physiological correlates of the loss of kinetoplast DNA. J Cell Biol 37:660–682

Storr SJ, Woolston CM, Zhang Y, Martin SG (2013) Redox environment, free radical, and oxidative DNA damage. Antioxid Redox Signal 20:2399–2408. doi:10.1089/ars.2012.4920

Stuart KD (1971) Evidence for the retention of kinetoplast DNA in acriflavine-induced dyskinetoplastic strain of *Trypanosoma brucei* which replicates the altered central element of the kinetoplast. J Cell Biol 49(189–195):1971

Trager W, Rudzinska MA (1964) The riboflavin requirement and the effects of acriflavin on the fine structure of the kinetoplast of *Leishmania tarentolae*. J Protozool 11:133–145. doi:10.1111/j.1550-7408.1964.tb01734.x

Wang MZ, Zhu X, Srivastava A, Liu Q, Sweat JM, Pandharkar T, Stephens CE, Riccio E, Parman T, Munde M, Mandal S, Madhubala R, Tidwell RR, Wilson WD, Boykin DW, Hall JE, Kyle DE, Werbovetz KA (2010) Novel arylimidamides for treatment of visceral leishmaniasis. Antimicrob Agents Chemother 54:2507–2516. doi:10.1128/AAC. 00250-10

Wilson WD, Nguyen B, Tanious FA, Mathis A, Hall JE, Stephens CE, Boykin DW (2005) Dications that target the DNA minor groove: compound design and preparation, DNA interactions, cellular distribution and biological activity. Curr Med Chem 5:389–408. doi:10.2174/1568011054222319

Witola WH, Atsuda A, Inoue N, Ohashi K, Onuma M (2005) Acquired resistance to berenil in a cloned isolate of *T. evansi* is associated with upregulation of a novel gene, TeDR40. Parasitology 131:635–646. doi:10.1017/S003118200500836X

Zuma AA, Cavalcanti DP, Maia MC, de Souza W, Motta MCM (2011) Effect of topoisomerase inhibitors and DNA-binding drugs on the cell proliferation and ultrastructure of *Trypanosoma cruzi*. Int J Antimicrob Agents 37:449–456. doi:10.1016/j.ijantimicag.2010.11.031

Zuma AA, Mendes IC, Reignault LC, Elias MC, de Souza W, Maçado CR, Motta MCM (2014) How *Trypanosoma cruzi* handles cell cycle arrest promoted by camptothecin, a topoisomerase I inhibitor. Mol Biochem Parasitol 193:93–100. doi:10.1016/j.molbiopara.2014.02.001